

ADVANCED THIN FILMS

Ultra-low Absorption Glasses and Optical Coatings for Reduced Thermal Focus Shift in High Power Optics

By Derrick Carpenter, Chris Wood, Ove Lyngnes and Nick Traggis

INTRODUCTION

Laser welding and cutting systems operate with high average power, and their performance is fundamentally limited by beam quality and stability of focus. Absorption in the transmissive elements of the optical system, both in the bulk materials and at the coated surfaces, has a detrimental effect on both of these parameters and is therefore to be minimized. Materials with extremely low bulk absorption are available, but the cost premium associated with these materials limits their use to only the highest-value applications. The antireflective coatings applied to the surfaces of these elements are another area of interest for the reduction of total absorption. Depending on the method used to deposit the AR coating, the absorption loss can vary by orders of magnitude, and in many instances it is the coating absorption that dominates the total absorption of the element. Scatter from the coating is also a potential issue as it can often represent a significant heat load to the opto-mechanical system, resulting in a purely mechanical focus shift; an ideal coating would maintain low scatter as well as low absorption.

We have thoroughly characterized the surface roughness and the bulk and surface absorption at $\lambda \sim 1\mu\text{m}$ on several candidate materials including both standard fused silica and low-absorption fused silica, both before and after AR coating, to assess the real-world performance that may be expected from them. Ion-beam sputtering (IBS) is selected as the deposition method for the AR coatings as they are known for durability under harsh operating conditions, spectral stability, and very low absorption and scatter losses¹. IBS coatings have been reported which exhibit sub-ppm absorption at 1064nm as part of the LIGO program² but only in relatively small quantities and at great cost. The aim of this work is to demonstrate that similar performance can also be achieved in a scalable, production setting and to provide information which will be beneficial in the

selection and specification of materials and coatings for high-power applications.

SAMPLE PREPARATION

One lot of fused silica (FS) substrates was fabricated from ground blanks into finished parts, 25.4 mm in diameter and 6.35 mm thick. This lot was composed of approximately 40 pieces each of Suprasil 3001, Spectrosil 2000, and Corning 7980 FS; upon receipt of the ground blanks, each piece was laser serialized on the barrel with a unique identifier to ensure proper identification throughout fabrication and coating. All parts were subjected to identical processing throughout the double-sided grinding and polishing steps comprising the standard PPC fabrication process for this class of part. Finished parts were inspected to meet PPC's typical specifications, including surface quality exceeding 10/5 scratch/dig per MIL-PRF-13830, peak-to-valley figure error $< \lambda/10$ at 632.8nm and wedge < 30 arc seconds.

ADVANCED THIN FILMS

Coating Run Number: S-2676, S-2677
Coating Job Number: WO13841, WO13842, WO13843

Approved by: J. Anton

AR 1064nm, 0° AOI, Scan of Witness

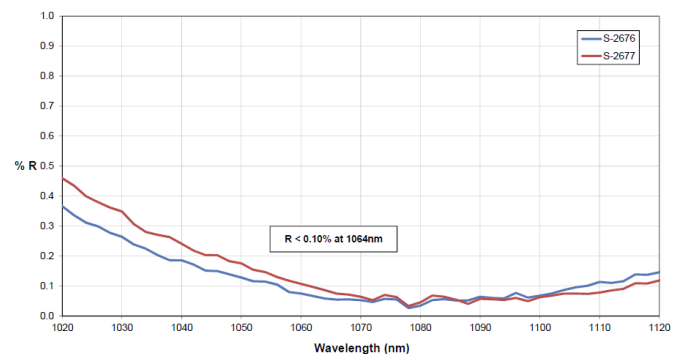


Figure 1. Measured AR coating scan showing $R < 0.1\%$ for each coated surface at 1064nm and 1070nm.

ADVANCED THIN FILMS

Three polished parts from each material group were chosen at random for additional metrology at this stage (the same three metrology samples of each material were used for all subsequent metrology for consistency). The RMS surface roughness of each part was measured using PPC's proprietary, NIST-traceable Nomarski microscope system which has a noise floor $<0.2 \text{ \AA}$ RMS. The surface- and bulk absorption of each sample was measured in multiple locations via photothermal common-path interferometry (PCI) using a 1070nm pump laser and a 632.8nm probe laser at normal incidence, with a detection limit of ~ 0.1 ppm for surface absorption and ~ 1 ppm/cm for bulk absorption. The physical basis for these measurements and actual measured results are presented below.

The polished parts were then coated on both surfaces with a high-performance, low-absorption anti-reflective (AR) coating deposited by PPC's ion-beam sputtering (IBS) process. In order to ensure that the results represent a fair assessment of production capability, this process was executed as a standard job, with no special attention paid by engineering or scientific staff during the actual coating process. The coating was designed for 1064nm incident illumination at normal incidence and is sufficiently broad that reflectance measured at 1070nm is essentially identical to that measured at 1064nm. The measured coating performance is shown in Figure 1, and indicates $R < 0.1\%$ at both 1064nm and 1070nm. Since the uniformity of the coating is well-controlled over all substrates by nature of the production process, a single measured value of reflectance is adequate to characterize the entire batch. The coated parts were re-inspected to ensure conformance to the expected standards of quality (e.g. flatness, wedge, and surface quality). After coating, the metrology samples were again measured for surface roughness and absorption to identify any effects which are attributable to the coating alone.

MEASUREMENT TECHNIQUE

Surface roughness was characterized using a NIST-traceable differential interference contrast (DIC) microscope system which was custom-built at PPC. Similar systems have been used for the quantitative characterization of surface roughness for decades, albeit with varying levels of absolute performance^{3,4}. In our particular system, linearly

polarized light (rotated 45° relative to the primary axes) passes through a Nomarski prism where its orthogonal components are transmitted with a small angular divergence, followed by a quarterwave plate which introduces a known retardance. The resulting small spatial shear at the image plane is approximately equal to the resolution of the objective lens and allows self-interference of the light which is reflected off the substrate surface after it passes through an analyzer. The resulting amplitude contrast is converted into absolute height variation, from which the RMS roughness can be calculated. A NIST-traceable 10-nm step height standard is used for absolute calibration of this system, and its noise floor is measured to be $<0.2 \text{ \AA}$ RMS. Our standard roughness measurement samples a $100 \mu\text{m} \times 100 \mu\text{m}$ region at a spatial wavelength of $1 \mu\text{m}$ (corresponding to the measured shear of the Nomarski prism in our system).

Absorption measurements were made at 1070nm using a photothermal common-path interferometer (PCI). The PCI technique is a type of photothermal deflection spectroscopy^{5,6} which uses a pump/probe configuration to measure both surface- and bulk absorption with excellent sensitivity and linearity. At the focus of the pump, local temperature rises in the presence of absorption. The wavefront of the probe beam is distorted in this region as a result of dn/dT and CTE (and possibly other, less common effects), and as the distorted wave propagates it generates a spherical wavefront. Meanwhile, the wavefront of the probe beam far from the thermal distortion remains planar and with distance the planar and spherical wavefronts interfere. Thus the small phase perturbation from the thermal distortion transforms into amplitude contrast which may be detected easily.

Such a system is shown schematically in Figure 2 - a 3mW, 632.8nm probe beam is used to detect the thermal effects of the absorbed 1W, 1070nm pump beam. The pump beam is focused to a $50 \mu\text{m}$ waist and chopped at ~ 400 Hz, allowing the use of a lock-in amplifier to isolate the corresponding signal from the photodiode (PD). The pump and probe beams are crossed at an angle of ~ 0.1 radians, resulting in a typical overlap of $\sim 0.5\text{mm}$, and the sample is scanned in three dimensions using computer controlled stepper

ADVANCED THIN FILMS

motors. This allows scans along all axes with moderate spatial resolution (50 μm along X and Y, 500 μm along Z), including Z-scans to isolate surface from bulk absorption and X-Y scans to map absorption as a function of position on the surface. Measurements are calibrated against a reference designed for surface absorption (Inconel deposited on fused silica) or bulk absorption (e.g. ND glass) to ensure accuracy. The lock-in amplifier ensures linearity over more than 7 orders of magnitude, allowing direct scaling from a $\sim 20\%$ reference down to a $< 0.01\text{ppm}$ measurement.

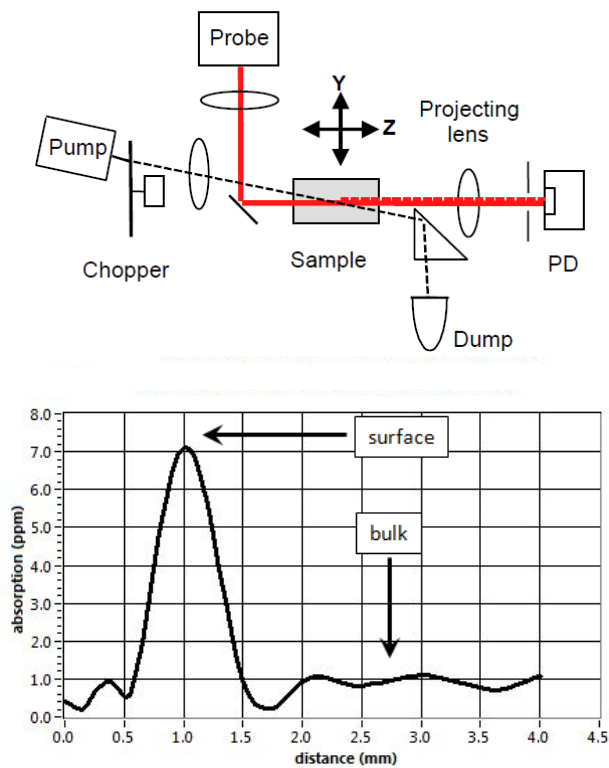


Figure 2. Schematic representation of a photothermal common-path interferometry system used to measure surface and bulk absorption (top) and typical data including both surface and bulk absorption (bottom).

All measurements were calibrated against the surface reference artifact (Inconel deposited on fused silica, $A=24.4\%$ measured by spectrophotometer). Because the coating is an AR and the pump is transmitted efficiently, we are able to simultaneously capture information about bulk absorption in the substrate. This is illustrated in Figure 2

which shows a typical measurement on a moderately low-absorbing coating deposited on Corning 7980 for a customer application. The 7 ppm peak is solely due to the coated input surface and has a full-width, half maximum (FWHM) corresponding to the interaction length of the pump and probe, which is $\sim 500\ \mu\text{m}$ in our system. If the angle between pump and probe were made larger, the FWHM would decrease, but the measured peak value would not change because the coating thickness is very small compared to the interaction length. In the region beyond the peak, there remains a non-zero signal of $\sim 0.9\text{ppm}$ which is due to the bulk absorption of the fused silica substrate. This value represents the aggregate bulk absorption associated with the entire interaction volume of the pump and probe, and is therefore directly affected by the interaction length. It may be converted to the typical units of ppm/cm by dividing the measured value by the interaction length. In this case, the result is $\sim 18\text{ppm/cm}$.

Using a 1W pump beam and reasonable detection times ($< 0.5\ \text{sec}$), our system has a detection limit of $\sim 0.1\ \text{ppm}$ for surface absorption and $\sim 1\text{ppm/cm}$ for bulk absorption. Typical uncertainty in the measured values is comparable to the detection limit.

ROUGHNESS RESULTS

Processed Nomarski images indicating measured RMS roughnesses are shown in Figures 3 and 4, corresponding to uncoated and coated parts, respectively. Measurements from the other parts are substantially similar, as expected since all parts were processed together during fabrication. All parts measured fall within a range of $1.0\ \text{\AA} \pm 0.1\ \text{\AA}$ RMS roughness, regardless of material type, as might be expected since they are all fused silica. The variation in roughness is typical for a fabrication lot of this type. A comparison of Figures 3 and 4 indicates that the deposition of the AR coating has a negligible effect on the measured roughness; this is expected since IBS is known to deposit highly dense, conformal coatings (in contrast to e-beam coatings which often develop structure which increases the roughness substantially). Scatter losses resulting from $\sim 1.0\ \text{\AA}$ RMS surfaces are expected to be well below 5 ppm for incident 1070nm illumination, indicating suitability for even the most scatter-sensitive systems.

ADVANCED THIN FILMS

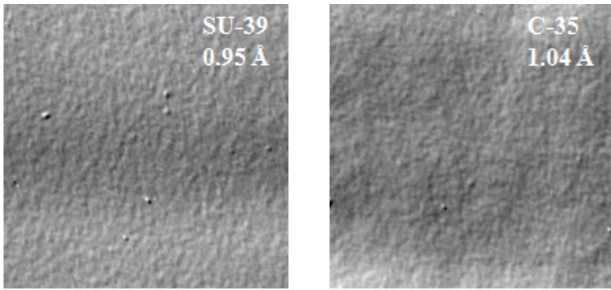


Figure 3. Nomarski images of uncoated parts. Field of view is 100 μm wide.

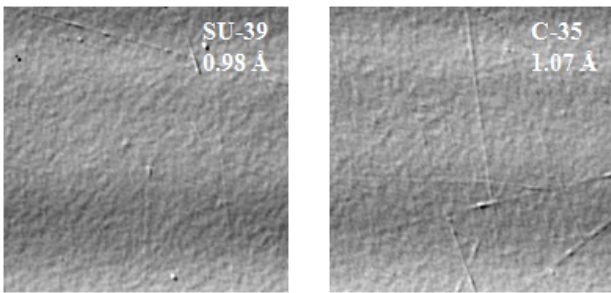


Figure 4. Nomarski images of coated parts corresponding to those shown in Figure 3. Field of view is 100 μm wide.

ABSORPTION RESULTS

All (9) of the metrology samples were tested for absorption at (3) locations near center, 1.5mm apart both before and after coating. Parts were scanned along the Z-direction with the pump/probe crossover starting and ending in free space on either side of the part. In the case of coated parts, parts were oriented such that the AR on the incident surface was from the same coating run. Figure 5 contains a summary of the data measured prior to coating, demonstrating the excellent consistency of the measured absorption across multiple locations on multiple parts. The peaks evident near the 1.2 and 5.3mm locations on the x-axis are the surface absorption associated with the entrance and exit surfaces, respectively, while the region between 2.5 and 4.5mm corresponds to the bulk absorption signal. There appears to be a small but consistent surface absorption component on the uncoated parts of both the 7980 and Spectrosil materials whose origin is not entirely obvious. Absorption resulting from residual polishing compound or cleaning solvents might be suspected, but if this were the

case, the same features should appear on all three types of material because they were processed identically. The absence of any measurable absorption on the surfaces of the Suprasil 3001 implies that the root cause is not the polishing/cleaning process itself.

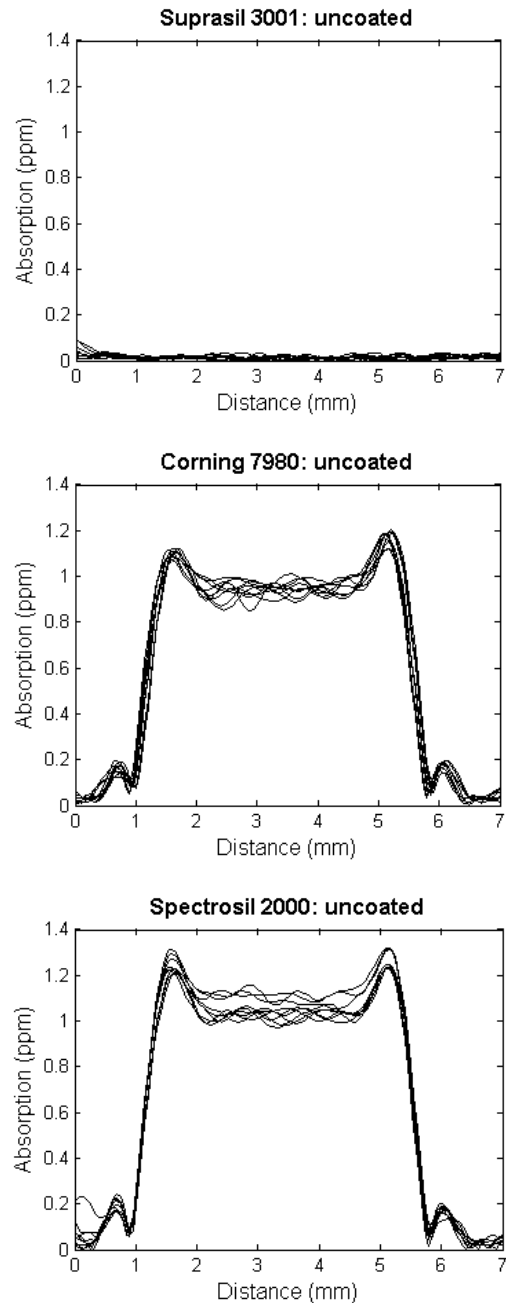


Figure 5. Measured absorption at (3) locations on each of (3) metrology samples per material. Suprasil absorption values (left) are below detectability limit.

ADVANCED THIN FILMS

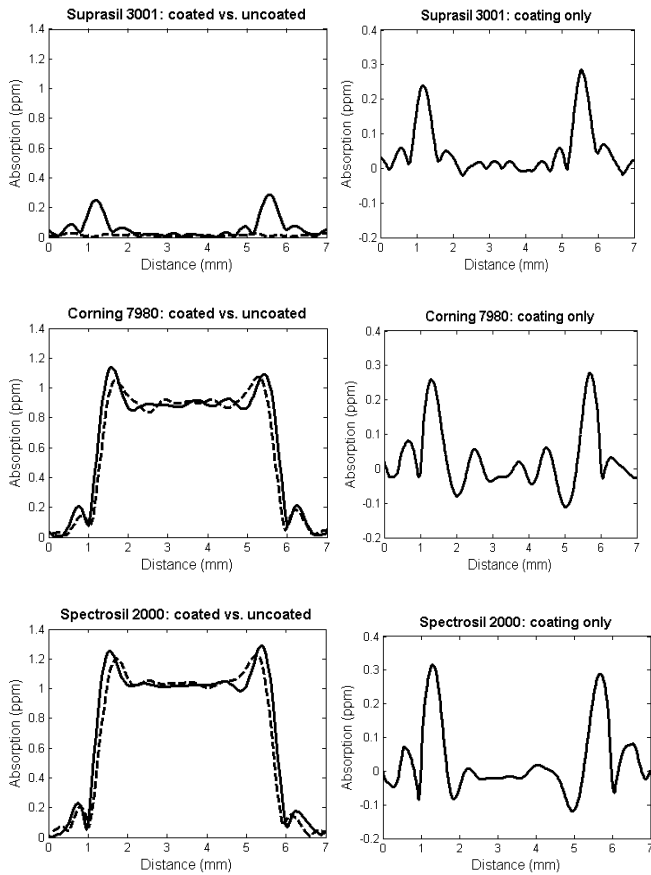


Figure 6. Top: Measured absorption before (dashed curves) and after (solid curves) AR coating on representative metrology samples of each material. Bottom: Absorption attributable to the AR coating only, obtained by subtracting the uncoated absorption from the coated absorption.

Figure 6 shows a comparison of measured absorption before (dashed curves) and after (solid curves) AR coating on representative metrology samples of each material, and indicates that the coating itself adds very little absorption to the part. For the Corning 7980 and Spectrosil 2000, the data have been scaled such that the bulk absorption is consistent between the uncoated and the coated measurements. This is a small correction (~5-7%) and well-justified since the measurements were made on the identical parts both before and after coating. After proper scaling, the effect of the coating itself is extracted by subtracting the uncoated absorption from the coated absorption, shown in Figure 6. The component of surface absorption which is directly attributable to the coating itself is ~0.3 ppm per coated surface and independent of the

substrate material, as one would expect since the coating is uniform over the entire coating lot and all parts were coated together. There is also very little difference between the two coated surfaces, indicating that IBS coating is a very stable and repeatable process.

Table 1 above contains a summary of the absorption data by material, including information from the manufacturers' data sheets for reference. The fact that the bulk absorption of Suprasil was below our detection limit is unsurprising, given its extremely low -OH content and the manufacturer's published bulk absorption at 1064 nm of < 1 ppm/cm. The measured bulk absorption in the other two materials appears consistent with the published typical -OH content, and would imply that this particular batch of Spectrosil likely has -OH content near the higher end of the specification as compared to the published bulk absorption of < 10 ppm/cm.

CONCLUSIONS

Several types of fused silica have been characterized for both surface and bulk absorption by PCI at 1070nm. Absorption correlates strongly with -OH content, as expected, and reinforces the fact that if ultralow absorption is absolutely critical, then low-OH material must be specified.

We have demonstrated that ultra-low absorption 1 μm AR coatings can be deposited by IBS under typical production circumstances. Such coatings add negligible scatter and contribute < 0.3 ppm per surface to the overall absorption of the element, independent of substrate material. This capability, in conjunction with low-OH substrate materials, allows routine production of transmissive elements with total absorption on order of a few ppm and expected scatter losses of < 10 ppm. Further, the opportunity arises to use moderately higher-OH materials (~1000 ppm instead of 1 ppm -OH) in thin lens applications where somewhat higher levels of absorption are acceptable. To first-order, the total absorption of an element is $A = (\text{bulk absorption}) \cdot \text{thickness} + 2 \cdot (\text{coating absorption})$, which simplifies to $A \sim (\text{bulk absorption}) \cdot \text{thickness} + 1 \text{ ppm}$ in the case of the AR coatings demonstrated here.

ADVANCED THIN FILMS

Material	Measured Bulk Absorption (this work)	Reported Bulk Absorption (from datasheet)	-OH content (from datasheet)	Metal impurities (from datasheet)	Surface Absorption (this work)		
					Uncoated	Coated	Coating only
Suprasil 3001	*	< 1 ppm/cm	< 1 ppm	< 1 ppm	*	0.25± 0.1 ppm	0.25± 0.1 ppm
Corning 7980	19 ± 0.6 ppm/cm	unavailable	800-1000 ppm	< 1 ppm	1.1 ± 0.1 ppm	1.2 ± 0.1 ppm	0.25± 0.1 ppm
Spectrosil 2000	21 ± 1 ppm/cm	< 10 ppm/cm	< 1200 ppm	< 1 ppm	1.2 ± 0.1 ppm	1.2 ± 0.1 ppm	0.25± 0.1 ppm

Table 1. Summary of measured absorption data by material along with supporting information. Reported bulk absorption, -OH, and impurities from respective manufacturers' datasheets and/or application notes.

In light of these results, further work is ongoing at PPC regarding the two-dimensional absorption behavior of polished and coated surfaces as well as the impact of coating design/function on absorption. A comparison of measured absorption attributable to a variety of IBS-deposited coatings (e.g. AR's, HR's, and polarizers) is presently underway.

ACKNOWLEDGEMENTS

The authors would like to express their gratitude to David Gritz and Michele Follmar of Heraeus USA for providing the raw material used in this study.

* Absorption is less than the detection limit.

REFERENCES

- [1] Baumeister, P.W., "Optical Coating Technology," SPIE Press, Bellingham Washington, 2004.
- [2] Flaminio, R., Franc, J., Michel, C., Morgado, N., Pinard, L., Sassolas, B., "A study of coating mechanical and optical losses in view of reducing mirror thermal noise in gravitational wave detectors," *Class. Quantum Grav.* 27(8) (2010).
- [3] Hartman, J.S., Gordon, R.L., Lessor, D.L., "Nomarski differential interference contrast microscopy for surface slope measurements: an examination of techniques," *Appl. Opt.* 20(15), 2665-2669 (1981).
- [4] Jabr, S.N., "Surface roughness measurement by digital processing of Nomarski phase-contrast images," *Opt. Lett.* 10(11), 526-528 (1985).
- [5] Kuo, P.K., Munidasa, M., "Single-beam interferometry of a thermal bump," *Appl. Opt.* 29, 5326-5331 (1990).
- [6] Bialkowski, S.E. [Photothermal spectroscopy methods for chemical analysis], John Wiley & Sons, New York, Chemical Analysis Series, 134 (1996)